WADC TECHNICAL REPORT 59-570

STOICHIOMETRY AND ELECTRONIC PROPERTIES OF PbTe

Edward Miller
Kurt K. Komarek
Irving B. Cadoff

New York University

DECEMBER 1959

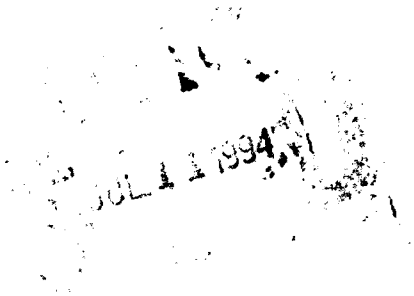

WRIGHT AIR DEVELOPMENT CENTER

NOTICES

When Government drawings, specifications, or other data are used for any purpose other than in connection with a definitely related Government procurement operation, the United States Government thereby incurs no responsibility nor any obligation whatsoever; and the fact that the Government may have formulated, furnished, or in any way supplied the said drawings, specifications, or other data, is not to be regarded by implication or otherwise as in any manner licensing the holder or any other person or corporation, or conveying any rights or permission to manufacture, use, or sell any patented invention that may in any way be related thereto.

- - - - -

Qualified requesters may obtain copies of this report from the Armed Services Technical Information Agency, (ASTIA), Arlington Hall Station, Arlington 12, Virginia.

- - - - -

This report has been released to the Office of Technical Services, U. S. Department of Commerce, Washington 25, D. C., for sale to the general public.

- - - - -

Copies of WADC Technical Reports and Technical Notes should not be returned to the Wright Air Development Center unless return is required by security considerations, contractual obligations, or notice on a specific document.

WADC TECHNICAL REPORT

STOICHIOMETRY AND ELECTRONIC PROPERTIES OF PbTe

Edward Miller
Kurt K. Komarek
Irving B. Cadoff

New York University

DECEMBER 1959

Aeronautical Research Laboratory
Contract No. AF 33(616)-3883
Project No. 7021
Task No. 70661

WRIGHT AIR DEVELOPMENT CENTER
AIR RESEARCH AND DEVELOPMENT COMMAND
UNITED STATES AIR FORCE
WRIGHT-PATTERSON AIR FORCE BASE, OHIO

200 – May 1960 – 36-1027

FOREWORD

This report was prepared by the Research Division, College of Engineering, New York University under USAF Contract No. AF 33(616)-3883. This contract was initiated under Project 7021, "Solid State Research and Properties of Matter", and Task 70661, "Effect of Internal Structure and Impurities on the Conductivity and Allied Phenomena in Solids" and was administered under the direction of the Aeronautical Research Laboratory, Directorate of Laboratories, Wright Air Development Center, with Mr. James W. Poynter acting as project engineer.

This report covers work done from December 1, 1956 to September 30, 1959.

ABSTRACT

Off-stoichiometric single crystals of PbTe were grown by the Bridgman technique at a solidification rate of 0.35 cm/hr. At this low solidification rate the crystals were longitudinally segregated, the composition at any point corresponding to that dictated by the solidus curve of the phase diagram. The phase diagram shows that PbTe has an off-stoichiometric melting point; the difference in concentration between the maximum melting point and the stoichiometric point being 0.002 atomic percent, with the congruent melting point on the tellurium rich side of the stoichiometric point. Stoichiometric PbTe is in equilibrium with liquid 0.41 weight percent rich in lead, the equilibrium temperature being 923.2°C. The solubility of both lead and tellurium in PbTe is restricted, the maximum lead and tellurium excess being 5×10^{-9} atoms/cm^3.

The crystals were cut into thin sections perpendicular to the growth direction and the slices homogenized to yield samples of different impurity concentrations of lead or tellurium. Resistivity, Hall coefficient, and thermoelectric power measurements were made as a function of temperature on three slices corresponding to stoichiometric, excess lead, and excess tellurium. High-temperature measurements could be made reproducibly with no loss of tellurium by coating the sample with Sauereisen No. 10, a room-temperature hardening cement. The results obtained were analyzed for the basic electronic parameters of the material. The high temperature results were brought into agreement with room temperature optical absorption data after correcting for vacancy generation at elevated temperatures.

The energy gap at absolute zero was calculated to be 0.24 eV, and has a temperature variation of $+ 2.5 \times 10^{-4}$ eV/°K. The mobility ratio is 2.2 + 0.15 and the electron and hole room temperature mobilities are 1170 and 500 cm^2/volt-sec respectively. The electronic effective mass was found to be 0.22 m and the hole effective mass 0.29 m.

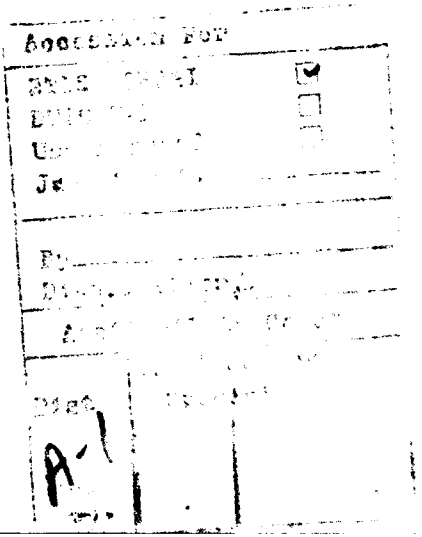

TABLE OF CONTENTS

LIST OF ILLUSTRATIONS

I. INTRODUCTION

During recent years increasing interest has developed in the class of materials known as semiconductors. A semiconductor can be defined as a material having a negative temperature coefficient of resistivity with resistivity values between approximately 10^{-3} and 10^{3} ohm-cm at room temperature.

The semiconductors which have been studied most are germanium and silicon, due to their many applications in transistors and rectifiers. However, it has been demonstrated (1) that the compounds of Types III-V and II-VI, that is, compounds formed between elements of the third and fifth columns and the second and sixth columns of the periodic table, also have semiconducting properties. These compounds are valence compounds and obey the empirical relationship derived by Mooser and Pearson (2) for semiconductors:

$$n_e/n_a + b = 8$$

where n_e is the number of valence electrons per molecule

n_a is the number of Group IV to VII atoms/molecule

b is the average number of bonds between the atoms of Groups IV to VII

Since lead acts as a divalent element in PbTe, this compound obeys the above rule.

PbTe is of particular interest for use as a thermoelement in thermoelectric generators. A thermoelectric generator can be defined as two different materials joined at one end which generate an emf when a temperature gradient is imposed along their length. It has been shown (3) that materials with high mean atomic weights should have good properties for use as thermoelements. PbTe falls in this category.

The investigation was centered on determining the values of the parameters that affect the electrical characteristics of the material. These are: the number of current carriers, the carrier mobility, the width of the forbidden energy gap in the compound, and the effective mass and sign of the charge carriers. These properties were obtained by growing single crystals of desired impurity concentrations and determining the electrical resistivity, Hall coefficient, and thermoelectric power of the crystals as a function of temperature. From these measurements the desired constants were calculated.

II. LITERATURE SURVEY

A brief review of the literature on PbTe is given below. This survey is not intended to be comprehensive, but rather to indicate the state of knowledge of the electronic properties of the compound, and also to serve as a summary of the

explain this, he concluded that the main impurity in both crystals was likely to be oxygen from air adsorbed on the crucibles' walls, and that this p-type impurity must be the cause of the failure to obtain n-type PbTe.

To remove all adsorbed gases, weighed quantities of lead and tellurium were placed in separate sidearms of a Y tube. The air was pumped out, hydrogen passed through the crucible, and the crucible heated to red heat. The lead was then melted into the vertical crucible (the bottom of the Y) and then heated to red heat. The hydrogen was then pumped out, and the tellurium melted onto the lead with hydrogen flowing once more. The hydrogen was pumped out again, the crucible sealed, and crystals grown. Lawson reported that n-type crystals of PbTe were grown in this way.

Putley (7) using the stoichiometric crystals grown by Lawson reported that in the intrinsic range these crystals had Hall coefficients indistinguishable from those of the polycrystalline samples studied previously (4). The values for the electrical conductivity, however, were greater by a factor of five to one hundred for the single crystals than for the polycrystalline specimens, resulting in mobilities much larger in the single crystal samples. The following compilation of data was reported:

Compound		PbS	PbSe	PbTe
energy gap eV		1.17		0.63
best mobility 290°K	elec.	800	1400	2100
cm^2/V-sec	holes	640	1400	840

Scanlon (9) pointed out that the high value of the energy gap for PbS reported by Putley did not agree with photoconductivity data and noted a source of error in Putley's interpretation of high-temperature resistivity and Hall measurements. In his experiments on single crystals of PbS, Scanlon observed that the concentration of lead or sulfur remained unchanged up to 500°K, as shown by reversibility of Hall effect and resistivity curves. On heating the crystal above this temperature irreversible behavior was noted due to vaporization of sulfur from the specimen. He avoided this vaporization by using Hall data on relatively pure samples below 500°K, and obtained the energy gap from the relation:

$$R = AT^{-3/2} e^{-E/2kT}$$

An energy gap of 0.37 eV was obtained for PbS by this method, which agreed closely with the optically determined value.

Brady (10) using Lawson's techniques for crystal growth attempted to prepare specimens of off-stoichiometric composition. He used both graphite and quartz crucibles, and found no correlation between the properties of the specimen and the crucible material.

Annealing the crystals after growth did not affect the properties of the specimens. Almost all of the outside surface of the stoichiometric samples was n-type, but this layer was present to a depth of only 0.002 to 0.010 cm. The bulk of the crystal was p-type and only the last 5 to 10 percent of the crystal was n-type throughout.

Non-stoichiometric samples were prepared, using Lawson's modified procedure. In samples containing excess lead, the portion that crystallized last was n-type as was the surface. Samples containing excess tellurium showed no n-type regions. Brady concluded that these results indicate that solid PbTe is not in equilibrium with liquid of exactly the same composition. The lattice constant of stoichiometric PbTe was found to be 6.4576 ± 0.0019 Å.

Silverman (11) prepared specimens of PbTe in single crystal form. He obtained crystals having conductivities ranging from 0.003 to 0.13 $(\text{ohm-cm})^{-1}$ and Hall coefficients of from +3 to -18 cm^3/coul. The mobilities were measured as 1500 $\text{cm}^2/\text{volt-sec}$ for electrons and 750 $\text{cm}^2/\text{volt-sec}$ for holes. During melting, lead segregated from the main body of the melt to the top, leaving the major portion p-type. A non-rectifying p-n junction was found along the bar.

Bloem (12) concluded that for PbS the introduction of excess lead into the crystal causes a sulfur ion vacancy. Of the two electrons given off by the lead atom, the first remains trapped at the positively charged sulfur vacancy, and the second one is so weakly bound to the vacancy that at room temperature it behaves as a free electron. Similarly, introduction of excess sulfur produced lead vacancies that trap one hole and give one free hole.

Putley (13,14) expanded his previous work and reported on lead sulfide, selenide, and telluride. He found, as before, that at high temperatures the Hall effect and electrical conductivity vary exponentially with temperature in a similar way for all specimens, but for every specimen a temperature exists below which the behavior of the Hall coefficient is characteristic of the specimen and is generally constant with temperature. Most specimens indicated negligible impurity activation energy, but some PbTe specimens showed evidence of impurity levels situated about 0.1 eV from either band.

The time taken to obtain the resistivity and Hall curves was five to eight hours. To check the reproducibility of the results a run was made on PbTe in which resistivity-temperature curves were obtained by heating a sample through various temperature cycles. The total time for each cycle was 15-20 minutes. No evaporization was noted until a cycle at 797°K was tried. Putley claimed that this showed that perfectly reversible results may be obtained up to 700°K.

In the most recent paper on thermal measurements on PbTe (15), crystals were grown by the Stockbarger method. Data were not taken in the intrinsic range for fear of irreversible evaporation, but by using low-temperature measurements of Hall coefficient, the energy gap was found to be 0.34 eV. Impurity ionization

energies were found to be very small.

The absorption spectra of PbTe have been obtained by various workers (16,17,18).

The most accurate determination of the energy gap from the absorption edge for PbTe, PbSe, PbS is that of Scanlon (19) who used micro techniques on samples as small as 600 x 50 microns. The crystal thicknesses ranged from 1 mm down to a few microns. The indirect transition energy was obtained by extrapolating the square root of the absorption coefficient vs photon energy to zero absorption, and the direct transition energy was obtained by extrapolation of the absorption coefficient squared vs photon energy.

The values obtained at 300°K were:

Material	Direct Energy Gap	Indirect Energy Gap
PbS	0.41	0.37
PbSe	0.29	0.26
PbTe	0.32	0.29

Smith (20) obtained the basic parameters for PbTe, PbSe, and PbS by comparing absorption, resistivity, and Hall coefficient, data, and used the constants that provided the best fit for all the data:

Compound	b	m_n/m	m_p/m	E eV
PbS	1.5	0.18	0.14	0.30
PbSe	1.3	0.15	0.17	0.22
PbTe	1.8	0.17	0.21	0.26

The phase diagram of the lead-tellurium system has been given in Hansen (30), who shows the solubility of lead and tellurium in PbTe to be extensive, the limits of solubility being 22-45 wt % tellurium. The limits were based on the magnetic susceptibility measurements of Endo (31). Pelzel (32) redetermined the solubility limits by determining the composition of the liquid in equilibrium with PbTe in two phase liquid plus PbTe alloys and confirmed the wide solubility limits. However, Brebeck and Allgaier (33) experienced difficulty in obtaining impurity concentration greater than 10^{19} cm^{-3}, much lower than would be expected for a compound having wide solubility limits.

Russian workers have observed (34) that if single crystals of PbTe containing excesses of Te are annealed at various temperatures and then quenched, a greater number of carriers are present in the samples than if they are slow cooled from the annealing temperatures.

They obtained an activation energy for the production of these thermally induced carriers to be 0.62 eV, assuming that the production of these impurities

follows a bimolecular law. They stated that the increase in number of carriers is due to the solution of tellurium in the compound from extraneous quiescent impurities.

They also found excesses of lead to have very little effect on the electrical properties of the compound unless substitution of monovalent cations for lead in the lattice were made. They claim that this results in a cation vacancy in which the excess lead atom can then dissolve and can then take part in the conduction processes.

The diffusion coefficient has been determined by observing the movement of a p-n junction along the length of a single crystal as lead was diffused into PbTe (35). Diffusion coefficient varying from 0.7×10^{10} to 3.5×10^{11} cm^2/sec were found over the temperature range of 532° to 773°K. An activation energy of 0.6 eV was calculated for the diffusion of Pb, 0.75 eV for Te.

This literature review indicates that there are several areas for research on the properties of PbTe.

The data of Brady (10), Silverman (11), and Lawson (5) indicate that PbTe has an off-stoichiometric melting point, but no quantitative measurements have as yet been made.

The large effect that evaporation of tellurium from PbTe at elevated temperatures can have on the electrical properties has only recently been understood (9), and one investigator (15) has avoided this error in PbTe by working at low temperatures. However, this leads to an inadequate knowledge of the high-temperature properties of the compound.

This investigation, therefore, had two main objectives: 1) to clarify the phase diagram of the Pb-Te system; 2) to obtain the thermoelectric properties of the compound at several selected impurity concentrations as a function of temperature and to obtain the basic electrical constants for PbTe from this data.

III. EXPERIMENTAL PROCEDURE

A. Crystal Growth:

The starting materials used were spectroscopically pure lead obtained from the American Smelting and Refining Company. A typical analysis is given in Table I.

Single crystals of PbTe were grown by the Bridgman technique. 150 g samples of desired compositions were weighed to $\pm$ 1 mg on an analytical balance and placed into quartz tubes which were evacuated to 1 micron and then sealed. In several cases the tube was heated to red heat with a torch to remove adsorbed

gases before the material was placed inside, and zone refined starting material used, but no consequent difference in the grown crystals was observed.

The capsule was sealed as close to the top of the material as possible in order to minimize the volume available for vaporization of tellurium. The sealed capsules were lowered through a nichrome-wound resistance furnace three feet long and 1-½ inches in diameter by a 1 rpm motor geared down to drive a rack at a rate of .35 cm/hr. The specimen was connected to the drive mechanism by a thin flexible wire running over several pulleys. The furnace temperature was held at 1080°C by means of a Variac and was recorded on a Weston temperature recorder. The temperature was found to vary less than 5°C during a run.

The resultant ingots were approximately 4 inches long and 1/2 inch in diameter. In several runs the capsules cracked during the solidification process, and the specimens became oxidized and were discarded. When the specimen was not oxidized, the ingots slipped easily out of the capsule, and had a clean, bright surface.

TABLE I

Spectroscopic Analysis of Starting Materials

Impurity	Concentration in Te	Concentration in Pb
Sb	nil	nil
Tl	nil	nil
Mg	nil	nil
Mn	nil	nil
Sn	nil	nil
Si	nil	nil
Cr	nil	nil
Fe	nil	0.0002
Ni	nil	nil
Bi	nil	0.0001
Al	nil	nil
Ca	nil +	nil
Cu	nil	0.0001
Cd	nil	nil
Zn	nil	nil
As	0.0001	nil
Se	0.0001	nil
Hg	nil	nil
Ag	nil	nil

B. Etching Crystals

An oxide staining procedure was used as a macroetch for observing any grain boundaries in the samples. To develop the boundaries, the specimens were polished down to 3/0 paper and then placed in a running vacuum in a furnace at 600°C for approximately five minutes to vaporize a very thin layer of tellurium from the surface. Air was then admitted to the system, the specimen being held at temperature for ten seconds to oxidize, and then water-quenched to stop the reaction.

Different grains become oxidized to different degrees, and grains were very clearly distinguished. No change in the bulk resistivity of the samples was observed due to this treatment.

C. Resistivity Scans

Resistivity scans along the length of the grown crystals were determined with a four-point apparatus. Four tungsten wires were inserted in holes in a Teflon block accurately spaced 0.050 inches apart. These probes were individually spring-mounted by means of spirals in the wires to permit individual motion where needed to compensate for irregularities on the specimen surface. The probes were pointed electrolytically (21).

The probes were pressed against the specimen's surface by lowering the unit onto the specimen by means of a rack and gear. Current was passed through the sample through the outer two probes, and then through a standard 0.01 ohm resistor. The voltage drop across the standard resistor was used to determine the current value. The inner two probes were used to determine the voltage drop across the sample.

Voltages were measured by means of a Rubicon Type B potentiometer and a spotlight galvanometer with a 0.5 uV sensitivity. The distance from the seed end of the sample was measured by means of a micrometer. Room temperature resistivities could be determined by this apparatus to an accuracy of 5×10^{-4} ohm cm.

D. Thermoelectric Scans

The tip of a 100-watt soldering iron was machined down to a point for use as a hot probe. The sample to be investigated was placed on a copper sheet, the probe pressed to the surface lightly, and the sign of the deflection was observed on a galvanometer connected to the base plate and the hot probe. The probe was moved along the specimen's length to obtain a scan of the sample.

E. Sectioning

The crystals were mounted on a porcelain plate with Apeizon wax, and slices into sections 0.1 inch thick perpendicular to the growth direction by a diamond cut-off wheel. These sections correspond to single crystals of various

impurity content of lead and tellurium.

The sections were then sealed into evacuated quartz capsules and homogenized at 850°C for 48 hours to remove any segregation before measurements were made. The capsules were less than 2 inches in length, and during the homogenization process the entire capsule was placed in the constant temperature zone of the furnace, so that no tellurium could be lost from the sample by condensation on cooler parts of the capsule. The resistivity of the two faces of the slices were determined after annealing, and were found to be the same within the limit of measuring error.

F. Resistivity vs Temperature:

Leads were welded onto the samples by electric resistance heating for resistivity determinations as a function of temperature. A brass plate was used as one welding electrode, and was connected to one output lead of a 5 ampere Variac. The other lead of the Variac was attached to a pair of tweezers, which was also used to manipulate the wire to be welded. A tapping key in the Variac output circuit permitted short current pulses to be sent through the circuit.

The surface to be welded must be oxide free, and the surface was freshly polished down to 3/0 paper immediately before welding. After several minutes standing in air, the probe generally would not make electrical contact with the sample, and the surface had to be repolished.

The slice was then placed on the brass plate, and the wire to be welded was touched gently to the surface at the point where welding was desired. The tapping key was depressed momentarily several times. The specimen-probe contact resistance heated the junction sufficiently to fuse the two together at the surface. Copper, silver, and gold wires were welded successfully, the bond being very strong; in tension the wire frequently broke before tearing out of the surface. These materials apparently form a low-melting eutectic with PbTe resulting in a high-strength bond. Three welding cycles of 5V applied for approximately 1/2 sec were used.

Four probes were attached to the specimens in a straight line on the surface. The distance between the probes was measured by using the graduated table of a metalloscope. Room-temperature resistivities of the samples were determined using the welded probes and the values were compared with the known four point resistivity. It was observed that if the spacing between the welded probes was greater than 0.050 inches, and the wires were less than 0.005 inches in diameter, then the resistivity values obtained by the two methods coincided.

For low-temperature resistivity measurements, the specimens were placed in a crucible around which a Nichrome heating element had been wound. This assembly was placed in an outer crucible which was then placed in a Dewar flask into which the coolant was also placed. The power input to the heater equalled the heat dissipated by the coolant at the desired temperature. Liquid nitrogen was used as the coolant for temperatures from 77°K to 186°K. Above this temperature range the liquid nitrogen evaporated very rapidly, resulting in appreciable temperature varia-

tions in the specimen compartment. Therefore, dry ice was used from 186°K up to room temperature. The temperature could be controlled to within 1°C for a period of one hour with this apparatus without the need for adding additional coolant.

No difficulties were encountered in obtaining measurements near room temperature, but as the temperature was lowered the probe-specimen contact resistance increased rapidly, and below -100°C the circuit resistance became so great that readings could no longer be taken with a potentiometer. The circuit resistance was determined using a Wheatstone bridge and was found to be very large and rectifying.

To obtain non-rectifying low-resistance probes, the contacts were pulsed with moderate voltages for short times. The contacts were welded in the usual manner, and then the Variac output was raised to 40-70 volts and the tapping key was depressed momentarily. When the pulsing was done fast enough, the probes remained welded firmly in place, and the circuit resistance remained below 20 ohms maximum and was non-rectifying. The pulsing could be done either at room temperature or after the specimen was placed in liquid nitrogen with similar results. The pulsing was generally done while the specimen was immersed in liquid nitrogen so that the low-temperature resistance before and after pulsing could be easily checked.

Using these pulsed contacts, measurements could be made easily from 77°K up to 300°K. The room-temperature resistivity of the samples was checked with the four-point probe apparatus after the low-temperature measurements and was found to be unchanged.

Since the weld strength of the silver probes is due to the formation of a low melting eutectic, for high-temperature measurements different probe materials must be used. 0.004 inch diameter molybdenum wires were found to form satisfactory welds up to 700°C, the highest temperature reached during the experiments. However, the strength of the weld is considerably less than when silver is used.

To prevent vaporization of tellurium from the surface of the samples at elevated temperatures, the specimens after welding were placed in 25-ml Pyrex beakers, and the beakers filled with Sauereisen cement and then baked at 80°C for 24 hours to harden the Sauereisen. The Sauereisen used (#10) is a low-temperature-hardening liquified procelain which is primarily used in the production of sparkplugs and forms a vacuum tight seal. The Sauereisen surrounding the specimen prevented tellurium from vaporizing from the surface and also provided mechanical support for the molybdenum wires.

To protect the molybdenum wires from oxidation, the assembly was placed in a Vycor tube, and running nitrogen was used as an inert atmosphere during the measurements. Resistivities could be determined by this procedure satisfactorily up to 700°C.

G. Thermoelectric Power vs Temperature:

Thermoelectric power vs temperature data were obtained by clamping the sample between two large copper blocks in which thermocouples were imbedded. A temperature gradient was established across the sample by placing the jig eccentrically either in a furnace or in a Dewar flask. The thermocouples were used to determine the temperature gradient across the specimens, and copper leads were used to obtain the emf generated by the specimen with respect to copper. To obtain a temperature gradient for room temperature measurements, a small strip heater was placed in one of the copper blocks. Gradients of 20° to 30°C were used for all measurements. Identical precautions were used for high-temperature measurements as were described for resistivity determinations.

H. Hall Effect vs Temperature:

The samples were cemented onto a lavite block with Dekhotinsky cement, and were then cut into rectangular shapes using a jeweler's saw. Current and voltage probes were welded onto the samples' edges using the techniques described previously. The Hall effect was determined for temperatures between 77°K and 700°K using the apparatus shown in Fig. 1.

The samples were placed in a Dewar flask between the poles of a D.C. electromagnet. For low temperature studies liquid nitrogen or a dry-ice and acetone mixture was placed in the chamber. To obtain intermediate and higher temperatures, a Nichrome resistance heater was used. The field strength was determined using a Rawlson rotating coil gaussmeter.

To eliminate Joule heating the procedure described in determining the resistivity was followed. To eliminate the Ettinghausen and Nernst effects, measurements were made with all possible combinations of field and current reversals as described by Olaf (22).

I. Room Temperature Absorption Spectrum:

A 1/8 inch thick slice of the single crystal was polished down sufficiently so as to be transparent in the infrared. The specimen was mounted on a flat steel plate with a hardened steel collar surrounding it to assure parallel polishing of the surface. Soft velvet polishing cloths were used, with 600 mesh alundum being used for the grinding operations, and 1 micron diamond paste as the final polishing material to produce a scratch free surface. The absorption spectrum was determined for several thicknesses between .4 to 150 mm over the wavelength range of 2 to 8 microns using a Beckman IR-2A spectrophotometer.

J. Thermal Analysis:

The liquidus line was obtained by thermal analysis. Samples to be investigated were sealed in quartz capsules having a central thermocouple wall. The capsules were small enough so that the entire length was at the same temperature, and thus no composition change could occur by either vaporization or con-

densation of tellurium on cooler parts of the capsule. The thermal analysis apparatus was constructed according to the specifications given by Roeser and Lonberger (23). A platinum/platinum-10% rhodium thermocouple was used. The thermocouple was calibrated against the melting points of copper, antimony, and zinc. The emf was obtained with a Rubicon type B potentiometer. The accuracy of measurement obtainable with this system is $\pm$ 0.5°C; the precision was better than 0.1°C.

K. Lattice Parameter:

The lattice parameter of various compositions were determined using the standard Debye-Scherrer X-ray technique. Seven twenty-five gram alloys covering the range 22 - 45 wt % tellurium were weighed to 1 mg and then sealed in vycor capsules in vacuum, heated above the melting point and then water quenched to prevent segregation during solidification. The samples were then homogenized in the capsule for 96 hours 25°C below the solidus temperature reported in Hansen. Powder patterns were taken using copper K radiation. The parameters were determined using the extrapolation of a_o vs $(\cos^2\theta / \sin^2\theta) + \cos^2\theta/\theta$.

IV. RESULTS

1. Phase Diagram

A. Introduction:

The electrical properties of any semiconductor depend on the concentration of the impurities in the sample. In this investigation the impurities of interest are excesses of lead and tellurium in stoichiometric PbTe. Therefore, to obtain crystals of varying composition, it is necessary to have accurate knowledge of the lead-tellurium phase diagram in the region near the stoichiometric point.

Furthermore, there is evidence in the literature that the congruent melting composition and the stoichiometric composition do not coincide, so that large errors in impurity content can occur during preparation if the actual maximum melting point composition is not known.

Several techniques were used to delineate the section of the phase diagram of interest. Thermal analysis could not be used to determine the solidus as the solidus temperature decreases very sharply with composition, and a thermal arrest cannot be observed accurately. However, the liquidus line near the maximum melting point must be practically a horizontal line, resulting in sharp arrests, and thermal analysis was used to delineate this curve.

The solidus line was obtained from the values of the electrical parameters of PbTe. The detailed description of the method used to obtain the boundaries is given below.

B. Thermal Analysis:

The liquidus temperature was determined for four compositions near the stoichiometric point by thermal analysis. The liquidus temperatures obtained are given in the following table:

TABLE II

Liquidus Temperatures in Pb-Te System

Composition	Liquidus Temperature ± .5°C
.4% excess Pb	923.2°C
.25% excess Pb	923.6°C
.08% excess Te	923.8°C
.28% excess Te	922.8°C

These values were used to plot the liquidus curve given in Fig. 6.

C. Resistivity Scans:

Resistivity scans of the crystals grown are shown in Figs. 2 to 5. Fig. 2 is the resistivity scan of a single crystal grown from liquid of stoichiometric composition. The resistivity of the sample is low in the initial portions to be solidified, but a sharp increase in resistivity is observed near the tail end of the specimen, and at approximately this point the thermoelectric power changes sign from p-type to n-type. The resistivity decreases after this peak toward the tail end of the specimen. The carrier concentration as a function of length along the crystal is shown in the bottom half of the figure. Hall measurements were obtained at several points along the length of the crystal, and the curve was calculated by assuming that the mobility of electrons and holes was a constant for the sample. The peak in the resistivity curve corresponds to a minimum in carrier concentration, the lowest measured concentration being 2×10^{16} carriers/cm^3. Above 10^{18}/cm^3 Hall coefficient measurements become very inaccurate and the curve cannot be drawn.

The explanation for this curve can be seen in the phase diagram shown in the figure. If we assume that the congruent melting point is to the tellurium side of the stoichiometric point on the diagram, then a specimen of stoichiometric liquid composition initially freezes out solid which is tellurium rich, or p-type. As solidification progresses, the solid approaches the stoichiometric composition and the resistivity rises. On further solidification, the solid rejected becomes lead-rich, the resistivity falls and the thermoelectric power changes to n-type.

The resistivity vs length curve for a second sample, corresponding to an overall liquid composition of 0.35 wt % excess lead is shown in Fig. 3. The curve

has a peak in resistivity corresponding to a minimum in carrier concentration near the center of the specimen. This is as expected, since the starting composition is closer to that of liquid in equilibrium with stoichiometric PbTe.

The resistivity of a third sample, of overall liquid composition of 0.40 wt % excess lead, is shown in Fig. 4. The resistivity peak is virtually at the seed end of the specimen, indicating that the liquid composition is very near to that in equilibrium with stoichiometric PbTe, and conversely that PbTe is in equilibrium with liquid of essentially 0.40 % excess lead.

A final sample, of 0.30 wt % excess tellurium is shown in Fig. 5. The resistivity continually decreases from seed to tail end, with no peak or discontinuity and remains always p-type in carrier sign. This would correspond to a sample on the tellurium rich side of the congruent melting point which segregates along the tellurium-rich solidus line.

The peak in resistivity should not occur at the stoichiometric point however, since the mobility of electrons and holes in PbTe are not the same. The stoichiometric point can be defined electronically as the composition where the number of electrons equals the number of holes. The composition where the maximum resistivity occurs can be found by the following analysis:

$$\sigma = ne\mu_e + pe\mu_p = (nb + p)e\mu_p \qquad (1$$

at any temperature: $np = n_i^2$ (2

$$\sigma = (b\ n_i^2\ p^{-1} + p)e\mu_p$$

$$d\sigma/dp = -b\ n_i^2\ p^{-2} + 1 = 0,\ bnp^{-1} = 1 \qquad (3$$

$$\text{therefore: } p = nb \qquad (4$$

That is, the maximum resistivity will occur where the number of electrons times the mobility ratio equals the number of holes. Therefore the two compositions will coincide if the mobility ratio is unity, but will have different values for all other cases. The difference between the hole concentrations of the two compositions can be calculated:

for the maximum resistivity composition $p_{max} = n_{max}b = (p_{max}n_{max}\ b)^{1/2} = n_i b^{1/2}$

for the stoichiometric composition $p_{stoich} = (n_{stoich}p_{stoich})^{1/2} = n_i$

$$p_{max} - p_{stoich} = n_i\ (b^{1/2} - 1) \qquad (5$$

Therefore, to obtain the difference between the stoichiometric and resistivity maximum compositions, n_i and b must both be known. The mobility ratio was found to be 2.2 and the room-temperature np product equal to 4.6×10^{31} (see section 2). Using these values in the above equations we find that the maximum

resistivity and the stoichiometric compositions differ by 2.3×10^{-5} atomic percent.

The maximum room-temperature resistivity obtainable in the lead-tellurium system occurs at the composition given by equation 5. The resistivity at this point can now be calculated from equation 1 using the mobility ratio and the np product values given above. The maximum resistivity was calculated to be 0.63 ohm-cm. Extrapolation of the resistivity vs length curves of Figs. 2 to 5 gives a maximum resistivity value of .3 ohm-cm, in excellent agreement with the calculated value considering the difficulty of extrapolating to the maximum value of a cusp.

D. Calculation of Solidus Line:

Sufficient information is now available to permit the shape of the solidus curve to be calculated. The liquidus is known from the thermal analysis data. The solidus line can be plotted directly from the liquidus if k_c (the solid to liquid solute concentration ratio) is known. k_c can be obtained by using the equation relating the concentration and fraction of an ingot solidified during directional solidification (24):

$$C = C_o k_c (1-g)^{k_c-1} \qquad (6$$

where C_o is the initial solute concentration in the melt

g is the fraction of the melt solidified

k_c is the ratio; solute in solid/solute in liquid

C is the concentration of solute at point g in the solid

The k_c value and the composition of the maximum melting point can be obtained from the above equation by using the data giving the variation of impurity concentration as a function of length of the grown crystals in Figs. 2 to 5. These curves are equivalent to C vs g curves and the distribution coefficient can be calculated using equation 6. The k_c value determined in this manner is $k_c = 0.013$ and the congruent melting point was found to be 0.002 atomic percent to the tellurium rich side of the stoichiometric point.

The approximation that k_c is independent of composition used in obtaining the solidus should be quite accurate in the small composition range around the congruent melting point. The liquidus curve is known from the thermal analysis measurements and the solidus can therefore be obtained using the value of k_c calculated above.

The completed phase diagram in the region near the congruent melting point is shown in Fig. 6. The congruent melting point occurs at 923.5°C at 0.002 atomic percent excess tellurium. The solidus temperature of the stoichiometric point is 923.2°C and the liquid in equilibrium with stoichiometric solid is 0.41 weight percent rich in excess lead.

E. Solubility Limits of PbTe

Hansen has published the phase diagram of the lead-tellurium system based on a compilation of reported data. The diagram has one intermetallic compound, PbTe, which is shown to have wide solid solubility limits extending from 22 to 45 wt % tellurium (31.4 to 57.1 at %). These limits were based principally on the magnetic susceptibility data of Endo. Pelzel redetermined the solubility limits on the lead rich side of the compound by measuring the relative areas of the two phases in samples annealed in the liquid + compound region. His data agreed with that of Endo.

However, there is reason to believe that this section of the diagram is incorrect. Recent studies of the semiconducting properties of PbTe (33) have indicated that addition of either lead or tellurium to PbTe does not produce samples having carrier concentrations greater than 5×10^{19} cm^{-3}. Assuming that each impurity atom results in one ionized charge carrier, this carrier concentration corresponds to a solubility range of less than 0.5 at %. In addition, Pelzel took the relative areas of the two phases proportional to the relative volumes, whereas the areas should be corrected for the different densities of the phases. The application of this correction results in a significantly narrower calculated solubility range. To resolve the discrepancy between these values, the solid solubility limits of the compound PbTe were re-investigated.

Eight 25 gr samples with compositions corresponding to 1, 3, 5 and 10 wt % excess lead and tellurium and two 100 gr samples corresponding to 15 and 65 wt % tellurium were prepared. The specimens were sealed in evacuated quartz capsules and melted at 950°C. The 1% excess Pb and Te and the 15 and 65 wt % Te alloys were homogenized for 96 hours at 450°C; the remaining specimens were annealed 50°C below the solidus temperature reported in Hansen. The specimens were then polished, etched with dilute HNO_3 and examined metallographically. All the samples were observed to be two phase, the second phase appearing at grain boundaries or as spheroidized inclusions in the grains. In the case of the tellurium rich specimens, the second phase was clearly a eutectic.

Debye-Scherrer powder diffraction patterns of the 1, 3, 5 and 10% excess samples were obtained using Cu K_α filtered radiation. The films were indexed as the B1 or NaCl structure. The calculated lattice parameter of PbTe was constant, for all the films, and the average of the eight samples gave $a_o = 6.460 \pm 0.0005$Å.

Lines due to excess lead or tellurium were very faint but could be clearly seen in all the films.

The percentage of the second phase present was determined by planimetry on the 15 and 65 wt % Te samples. The relative areas of the two phases on a 100 magnification microphotograph were corrected for the differences in density of Pb, Te and PbTe, and were then taken as proportional to the relative volumes of the two phases. The corrected relative volumes agreed with a phase diagram having low solubility of both lead and tellurium in lead telluride.

Since planimetry gives correct volume ratios only if the grains of the two phases are randomly distributed, the result was checked by determination of the density of the two specimens by weighing in air and in water. The specimens were broken into small pieces to eliminate any internal porosity. Any adherent air bubbles were then removed by vigorous shaking under water for several hours. The density of lead (11.34 g/cm^3) and of tellurium (6.25 g/cm^3) was taken from the International Critical Tables and that of stoichiometric PbTe (8.25 g/cm^3) calculated from the lattice parameter. For the 15 wt % Te samples, the density assuming no solubility was calculated to be 9.89 g/cm^3; the observed density was 9.86 g/cm^3. For the 65 wt % Te alloy, the density calculated for the case of no solubility was 7.24 g/cm^3; the observed density was 7.22 g/cm^3. These results are consistent with those of planimetry.

It can be concluded that the solubility limits of PbTe are quite narrow, and that the electrical measurements previously cited accurately define the phase diagram. The maximum solid solubility of both lead and tellurium in PbTe can therefore be placed in the range of 0.2 at %.

2. Electronic Properties

A. Introduction

To determine the electronic properties of PbTe, three slices cut from single crystal 1 were studied extensively. Measurements were made on sections corresponding to stoichiometric, excess lead (n-type), and excess tellurium (p-type), all having carrier concentrations less than 10^{18}/cm^3.

The resistivity, Hall coefficient, and thermoelectric power of the three samples investigated are shown as a function of temperature in Figs. 7 to 15.

Sample 3 was cut from the tellurium-rich section of the ingot and is p-type, as was determined from the sign of the Seebeck and Hall coefficients. Sample 14 was the slice with the highest resistivity after homogenization and was taken as being the slice closest to stoichiometric in composition. The sign of the majority carriers was also found to be positive. Sample 19 was cut from the tail end of the specimen, corresponding to excess lead and is n-type.

The intrinsic electrical properties of a semiconductor are largely determined by the width of the forbidden energy gap and by the effective mass and the mobilities of the current carriers. The inclusion of impurities in the material alters the low-temperature behavior from that of a pure semiconductor.

The methods by which these parameters are calculated from the Hall, resistivity, and thermoelectric power data obtained is discussed below.

Three methods were used to determine the energy gap:

1. Determination from the slope of the resistivity-temperature curve.

2. Determination from the variation of carrier densities as a function of temperature.

3. Determination of photon energy necessary to excite across the forbidden gap.

B. Resistivity-Temperature Determination of Energy Gap:

The relation between resistivity and temperature in the intrinsic conductivity range of a semiconductor is:

$$\rho = 2e\,(2\pi\,kT/h^2)^{-3/2}\;\;(m_n\,m_p)^{-3/4}\;\;e^{E/2kT}\;\;(\mu_n+\mu_p)^{-1}$$

The calculation of the energy gap is based on the assumption that the resistivity variation with temperature can be simplified to:

$$\rho = Be^{E/2kT}$$

where $E = E_o + \beta T$

β and B are constants.

Since B contains a $T^{-3/2}$ term and a mobility term which is temperature dependent, B can be independent of temperature if mobility varies as $T^{-3/2}$.

Differentiating the logarithm of the resistivity with respect to 1/T in this simplified equation gives:

$$E_o = 2k\;\;\frac{d(\ln\rho)}{d(1/T)}$$

Hence, the slope of the ln ρ versus 1/T is a measure of the energy gap. The above equation implies that the mobility of the carriers varies with temperature as $T^{-3/2}$ (in order for B to be independent of temperature). The $T^{-3/2}$ variation of mobility with temperature is that predicted for lattice scattering by phonons in the acoustical mode, and is obeyed by germanium and silicon at room temperature. Attempts have been made to explain other power dependence by assuming that phonons can be scattered by optical modes as well as the acoustical modes of vibrations, thus altering the temperature dependence of mobility. There is also a small contribution to the temperature dependence of mobility by electron-hole scattering at high carrier densities. The

amount of this contribution has also been calculated using a modified impurity scattering derived by Conwell (25). Hole mobilities in germanium were found to vary with as high as the -5/2 power of temperature at very high temperature, and Shogenu and Uchiyama (15) have found PbTe to obey this relationship at all temperatures.

The logarithm of the resistivities of the samples as functions of the reciprocal temperature are given in Fig. 7, 10 and 13. The intrinsic resistivities are replotted on an expanded scale in Fig. 16. The plots are straight lines in the intrinsic range, with slopes corresponding best to 0.35 eV. The intrinsic resistivities are reproducible after heating, cooling, and reheating of the specimens, indicating that tellurium vaporization up to 700°C is negligible when a Sauereisen coating is used.

The fact that the intrinsic resistivity curve is a straight line indicates that variations in resistivity due to temperature dependence of mobility and position of the Fermi level are not very significant compared to the exponential thermal excitation of electron-hole pairs, which appears to be the controlling factor at high temperatures.

C. Carrier Concentration vs Temperature Determination of Energy Gap:

Although the method described above shows there is no simple relation between 1/T and the energy gap, if the product npT^{-3} is formed for a non-degenerate semiconductor a function is obtained which will lead to the desired relation exclusive of the mobilities and position of the Fermi level (26). This product is:

$$npT^{-3} = 4(2\pi k/h^2)^3 \quad (m_n m_p)^{3/2} \quad e^{-E/kT} \qquad (7$$

The activation energy E can then be obtained from the slope of a plot of the log of npT^{-3} against 1/T.

To calculate the value E by this method the electron and hole concentrations must first be obtained from the Hall coefficient data. The Hall coefficient in the intrinsic region is given by:

$$R = - \frac{3\pi (nb^2 + p)}{8e (nb + p)^2} \qquad (8$$

In the exhaustion range, that is, at temperatures at which all impurities are ionized and a negligible number of valence electrons are excited into the conduction band, the Hall coefficient equation for p-type samples reduces to:

$$R = \frac{+3\pi}{8ep} \qquad (9$$

From the condition of electrical neutrality we have:

$$p = n + N_a \qquad \text{(for p-type)} \qquad (10$$

where N_a = the number of acceptor impurity atoms/cm^3.
Therefore, if the mobility ratio is known, n and p at any temperature can be calculated from equations 7,8,9. The assumption inherent in these equations, that the mobility ratio is constant with temperature, is made without complete justification. However, if n and p are calculated from the equation using this assumption and a straight line is obtained in a plot of log npT^{-3} against $1/T$, it is reasonably sure that b is constant over the temperature range investigated.

Determination of the mobility ratio is almost invariably performed in p-type material by determining the ratio of the maximum value of the Hall coefficient in the intrinsic range to the value of the Hall coefficient in the extrinsic range (27).

However, this method cannot be used in n-type material, since the Hall coefficient continually decreases to zero and does not have a maximum. Since it is desirable to have independent mobility ratio determinations in all the samples, the method devised by Hunter (28) was used. This method has the added advantage that there is no possibility of error due to the difference between the Hall mobility and the drift mobility. Hunter has shown that the mobility ratio is determined by the intersection of the extrinsic and the intrinsic resistivity curve extrapolations. The mobility ratio can then be given by:

$$b = \frac{1}{r-1} - r \qquad \text{(p-type)} \qquad (11$$

$$\frac{1}{b} = \frac{1}{r-1} - r \qquad \text{(n-type)} \qquad (12$$

where r is the ratio ρ_e / ρ_o where ρ_e is the resistivity of the extrinsic line extrapolated to the intersection of the intrinsic and extrinsic lines, and ρ_o is the actual resistivity at the same temperature. However, since the ratio of the two resistivities is used, the resistivity in the transition region must be determined very accurately. Resistivities could be determined in this temperature range to 10^{-3} ohm-cm, corresponding to a mobility ratio error of $\pm$ .05.

A difficulty associated with this procedure is the determination of a satisfactory method of extrapolation. The intrinsic line can be extrapolated without difficulty since it is a straight line. However, the extrinsic line is decidedly curved. Hunter (28) suggests extrapolation assuming that the mobility is a simple power function of temperature, and this procedure was used in this investigation. However, the mobility versus temperature curves found for PbTe do not fall on a simple power function plot very well, and it is estimated that an error in mobility of $\pm$ 0.1 was introduced due to the uncertainty in the extrapolation.

The mobility ratio determinations in the transition range are shown in Fig. 17, 18, 19. The average value of the mobility ratio was determined to be 2.25 ± 0.25.

Using this value, n and p were calculated by means of equation 8. The log npT^{-3} is plotted for sample 14 vs $1/T$ in Fig. 21. Analysis could not be performed on samples 3 and 19 since the Hall coefficient of these samples is so low that variations of Hall coefficient with temperature could not be accurately followed. The slope of the curve for sample 14 was found to correspond to 0.35 eV, in good agreement with the slope of the resistivity vs temperature.

D. Determination of Optical Energy Gap:

The energy gap can be determined by the interaction of photons with the electrons in the valence band. At photon energies below that of the forbidden gap there will be no excitation and the only interaction will be weak absorption by any free carriers in the sample. At photon energies equal to that of the forbidden gap the absorption coefficient will rise sharply.

Direct transitions from the valence to the conduction band can occur provided that the wave number does not change during the transition. In such transitions it has been shown (19) that the absorption coefficient is proportional to the square root of the photon energy. In indirect transitions, where phonon-electron interactions occur, the absorption coefficient is lower and is proportional to the square root of the photon energy.

The direct energy gap can therefore be obtained by extrapolating the absorption coefficient squared vs photon energy to zero energy; the indirect gap can be obtained from a plot of the square root of the absorption coefficient vs the photon energy (19). The extrapolation is shown in Fig. 22. The energy gap for direct transitions is 0.32 eV.

E. Determination of Carrier Mobilities:

The mobilities of the carriers can be found using the calculated values of p and n. The ratio of mobilities is assumed a constant with temperature. The resistivity is given by:

$$\rho = (ne\mu_n + pe\mu_\rho)^{-1} \qquad (13$$

This may be simplified in the extrinsic range to:

$$\mu_n = (\rho en)^{-1} = \frac{-8R}{3\pi\rho} \quad \text{for n-type material} \qquad (14$$

and

$$\mu_\rho = (\rho e p)^{-1} = \frac{8R}{3\pi\rho} \quad \text{for p-type material} \qquad (15$$

In the transition region between the intrinsic and extrinsic ranges, where both n and p are appreciable and not equal, we have:

$$n = 8/3\pi\rho e(n + p/b) \qquad \text{for n-type material} \qquad (16$$

and

$$p = 8/3\pi\rho(p + bn)\, e \qquad \text{for p-type material} \qquad (17$$

Fig. 20 shows the calculated majority carrier mobilities as a function of temperature for samples 3, 14, and 19. The mobilities decrease with increasing temperature, the hole mobility of Specimen 3 decreasing more rapidly than that of the purer Specimen 14. At approximately room temperature the mobilities of the two p-type samples approach each other and the mobility of the n-type sample approached the value of $b\mu_p$.

It therefore appears that the mobilities above 200°K can be considered as being determined primarily by lattice scattering which is independent of impurity concentration, while at lower temperatures the scattering is largely due to impurity ions. However, the mobility of the stoichiometric sample 14 should be higher than that of the impure sample 3 if this simple model were correct, and in order to explain the difference it is necessary to assume that the intrinsic sample is highly compensated, possibly with lead atoms sitting in tellurium lattice sites and tellurium atoms sitting in lead lattice sites.

F. Determination of Effective Masses:

The effective masses of the charge carriers can be obtained from the Seebeck coefficients values in the extrinsic region. In this region the Seebeck coefficient is given by:

$$S = \pm \frac{k}{e}\left[2 - \ln\left\{\frac{nh^3}{2(2\pi m \cdot kT)^{3/2}}\right\}\right] \qquad (18$$

This equation assumes lattice scattering is predominent, which is true at room temperatures and above. Substituting the room temperature values for the Seebeck coefficient and the number of carriers for samples 3 and 19 we obtain:

$$m_n = 0.22\ m$$

$$m_p = 0.29\ m$$

G. Determination of Temperature Variation of E_o:

The position of the bands and the band edges is a function of temperature. This can be partially explained by the shift in the energy levels by the volume expansion of the lattice with temperature and excitation of lattice vibrations. The change in gap has been shown to be a linear function of temperature in many semi-

conductors (1). We can therefore give the variation of energy gap with temperature by the equation:

$$E = E_o + \beta T \qquad (19$$

β can also be determined from the Seebeck coefficient vs temperature measurements. In the intrinsic range the Seebeck coefficient can be given by (29):

$$S = \frac{-k}{e}\frac{(b-1)}{(b+1)}\left[\frac{E_o}{2kT} + 2 + \beta/2k - \frac{2}{5}\ln b\right] \qquad (20$$

Substituting $E_o = 0.24$ eV (see Section V) and $b = 2.2$ into this equation and using the Seebeck coefficients of Figs. 8, 11, 14 we obtain:

$$\beta = 2.5 \times 10^{-4} \text{ eV/°K}$$

V. DISCUSSION

The experimental results show that the optical energy gap for indirect transitions does not agree with the activation energy measured thermally. The original discrepancy between thermal values and optical values were shown by Scanlon (9) to be due to the vaporization of tellurium from the specimen at elevated temperatures. However, in the present investigation vaporization was effectively prevented, as is shown by the reproducibility of the resistivity curves on repeated heating and cooling cycles. Therefore, it appears that mechanisms must be present for carrier production in the thermal measurements which are not available in the optical measurements.

Recent Russian work by Koval'chick and Maslakovets cited in the literature survey has shown that specimens which are quenched after elevated temperature anneal have a greater number of carriers than specimens which are slowly cooled from the annealing temperature. Assuming a bimolecular reaction, the activation energy determined for this thermal production of carriers was 0.62 eV. They concluded that the production of carriers at the annealing temperature is most probably caused by the solution of excess quiescent impurity atoms in lead telluride; or, when the composition of the specimen is exactly stoichiometric, by dissociation of the compound, and in this case the slope will characterize the energy of dissociation.

However, it appears unlikely that this thermal carrier generation is caused by the solution of excess atoms. Such solution must have as one step a diffusion process, and the slope of the excess carrier concentration - temperature curve is much smaller than the slope expected for a reaction involving diffusion. In addition, there is no reason for assuming a bimolecular reaction. If the calculation is based on a unimolecular reaction, the activation energy obtained is 0.32 eV.

Pilat obtained the values of 0.62 eV and 0.75 eV for diffusion of lead and tellurium respectively in PbTe. The diffusion activation energy consists of two parts, the jump activation energy and the vacancy production energy. The observed slope of 0.32 eV for carrier generation is therefore approximately what would be expected for the slope of the vacancy concentration-temperature curve. The small energy calculated to be necessary to form a vacancy in PbTe as compared to most other materials is probably due to the high polarizability of the lead and tellurium atoms, which results in relaxation of the Coulombic forces. Production of vacancy pairs will occur at roughly twice this energy value and is also to be expected. However, since PbTe is only partly ionic, it is not necessary that anion and cation vacancies be produced in equal concentrations, and it is likely that a greater number of lead than tellurium vacancies will be generated due to the differences in atomic radii.

Several mechanisms exist by which the vacancies existing in the lattice can produce current carriers. A vacancy created by the removal of the more electropositive lead atoms will tend to attract electrons, resulting in a level in the forbidden energy region close to the valence band. Conversely, a vacancy on the more electronegative tellurium lattice tends to lose electrons and produces an additional level near the conduction band. Second ionizations for each type of imperfection are also possible. Such levels will compensate each other at low temperatures if the concentration of the two types of vacancies are the same. As mentioned above, however, more lead vacancies should exist at all temperatures. Another possibility is the production of anti-structure disorder in the crystal. Anti-structure disorder, that is, lead atoms sitting at tellurium sites and tellurium atoms sitting at lead sites should exist to some extent in the compound. With increasing temperature the concentration of anti-structure disorder should increase due to the accompanying increase in entropy. The tellurium ion on a lead site will form an imperfection that will tend to donate electrons, and will form a level near the conduction band. The lead ion on the tellurium site will tend to accept an electron and will form an acceptor level near the valence band. Reaction with vacancies permits different concentrations of the two anti-structure reactions to occur.

The third possible mechanism for carrier generation is vacancy pair separation. Lead vacancies are negatively charged and tellurium vacancies positively charged with respect to the surrounding crystal and will attract one another. When a vacancy pair has been formed, the resultant double vacancy is not charged, and does not interact with the charge carriers. However, with increasing temperature the number of vacancy pairs becomes smaller and the constituent vacancies regain apparent charges. The lead and tellurium vacancies can then form donor and acceptor levels as mentioned before.

Whatever the mechanisms for the production of these additional carriers, measurements taken at elevated temperature will detect carriers generated by two distinct mechanisms: 1) the generation of electron-hole pairs across the energy gap and, 2) production of excess carrier at the elevated temperature. Optical measurements at room temperature however, will only observe carriers which are excited across the energy gap. Therefore, to obtain the number of carriers excited across the energy gap from the thermal measurements the excess concentration must be subtracted from the total carrier concentration determined. Fig. 23 is a plot of the carrier concentration as obtained from the value of Fig. 21 and the thermal carrier concentration determined by Koval'chick. Since Koval'chick gave only a small graph of his values for carrier production, it is difficult to reproduce his data accurately, and some error in replotting is inevitable. The difference curve should yield the actual electron-hole equilibrium concentration. From this plot the bandgap at 0°K is found to be 0.24 eV, in much better agreement with the optically determined value than is the uncorrected value. The calculated electron-hole equilibrium concentration is added to the excess carrier concentration in the bottom graph of Fig. 23 to yield the total number of carriers. It can be seen that the log of the total carrier concentration is a straight line function of the reciprocal temperature only at intermediate temperatures. At high temperatures the excess carrier concentration predominates, while at lower temperatures the electron-hole pair production is predominant. The low temperature region is not observable since impurity conduction becomes signicant, and the high temperature region was not observed due to experimental difficulties.

Free vaporization of the constituents from the specimen must result in a large concentration of vacancies forming in the sample. This will result in the excess carrier concentration line being pushed to values higher than the equilibrium values, and these excess carriers will then be predominant. This is evidenced by the work of Putley (8) who obtained 0.63 eV when such free vaporization was permitted to occur.

VI. BIBLIOGRAPHY

1. Welker, H. and Weiss, H., "Solid State Physics," New York, Academic Press (1956) 1st Edition, Volume 3, pp 1-79.

2. Mooser, E. and Pearson, W. B., Chemical Bond in Semiconductors, Phys. Rev., 101 (1956) 1608-9.

3. Goldschmid, H. J. and Douglas, R. W., Application of Peltier Effect to Refrigeration, Brit J. Appl. Phys., 5 (1954) 386-9.

4. Chasmar, R. P. and Putley, E. H., "Semiconducting Materials," London, Buttersworth Sci. Pub. (1951), 1st Edition, 208-23.

5. Lawson, J., A Method of Growing Single Crystals of PbTe and PbSe, J. Appl. Phys. 22 (1951) 1444-7.

6. Lawson, J., Oxygen Single Crystals of PbSe, PbTe and PbS, J. Appl. Phys., 23 (1952) 495-7.

7. Putley, E. H., Electrical Conductivity of PbS, PbSe, PbTe, Proc. Phys. Soc., 65B (1952) 388.

8. Putley, E. H., Intrinsic Conduction in PbS, PbSe, PbTe, Proc. Phys. Soc., 65B (1952) 993.

9. Scanlon, W. W., Interpretation of Hall Effect and Resistivity Data in PbS, Phys. Rev., 92 (1953) 1573-4.

10. Brady, E. L., Preparation and Properties of PbTe, J. Elec. Soc., 101, (1954) 466-73.

11. Silverman, H. J., and Levenstein, H., Electrical Properties of Single Crystals and Thin Films of PbSe and PbTe, Phys. Rev., 94 (1954) 871-6.

12. Bloem, J., Controlled Conductivity in PbS Single Crystals, Philips Res. Rep., 11 (1956) 273-366.

13. Putley, E. H., Hall Effect, Electrical Conductivity and Magnetoresistance Effect in PbS, PbSe, and PbTe, Proc. Phys. Soc., 68 (1955) 22-34.

14. Putley, E. H., Thermoelectric and Galvanomagnetic Effects in PbSe and PbTe, Proc. Phys. Soc., 68 (1955) 35-42.

15. Shogenji, K. and Uchiyama, S., On Electrical Resistivity and Hall Coefficient of PbTe Crystals, J. Phys. Soc. Jap. 12 (1957) 431.

16. Moss, T. S., Temperature Variation of the Long-wave Limit of Infrared Photoconductivity in PbS and Similar Substances, Proc. Phys. Soc. B62 (1949) 741-8.

17. Avery, D. G., Further Measurements on the Optical Properties of PbS, PbSe and PbTe, Proc. Phys. Soc. 67 (1954) 2-8.

18. Moss, T. S., Interrelation Between the Optical Constants for Silicon, Proc. Phys. Soc., 66 (1953) 141-4.

19. Scanlon, W. W., Recent Advances in the Optical and Electronic Properties of PbS, PbSe, PbTe and their Alloys, J. Phys. Chem. Solids, 8 (1958) 423-8.

20. Smith, R. A., Electronic and Optical Properties of the Lead Sulfide Group of Semiconductors, Physica, 20 (1954) 910-29.

21. Pfann, W. G., An Electrolytic Method for Pointing Tungsten Wires, Metals Tech., Tech. Pub. 2210, June 1947.

22. Lindberg, O., Hall Effect, Proc. I.R.E. (1952) 1414-19.

23. Roeser, W. F. and Lonberger, S. T., Methods of Testing Thermocouples and Thermocouple Materials, National Bureau of Standards, Circular 590, Feb. 6, 1958.

24. Pfann, W. G., Principles of Zone Melting, Trans. A.I.M.E. (1952) 747-53.

25. Morin, F. G. and Maita, J. P., Conductivity and Hall Effect in the Intrinsic Range in Ge, Phys. Rev., 94 (1954) 1525-9.

26. Morin, F. G. and Maita, J. P., Ibid.

27. Breckenridge, R. A. et al., Electrical and Optical Properties of Intermetallic Compounds, Phys. Rev., 96 (1954) 573-5.

28. Hunter, I. P., Current Carrier Mobility Ratio in Semiconductors, Phys. Rev., 91 (1953) 579-81.

29. Johnson, V. A. and Lark-Horovitz, K., Theory of Thermoelectric Power in Semiconductors with Applications to Germanium, Phys. Rev., 92 (1953) 226-32.

30. Hansen, M., "Constitution of Binary Alloys," McGraw Hill (1958) 2nd Edition.

31. Endo, H., Science Repts. Tohsku Univ. 16 (1927) 209.

32. Pelzel, E., Metall. U. Tech. (1956) 717.

33. Brebeck, R. F. and Allgaier, R. S. and Hammond, G. L., Bull. Am. Phys. Soc. 4 (1959) 134.

34. Koval'chick, T., Maslakovets, Yu., "The Effect of Impurities on PbTe," Shur Tekh Fiz 26 (1956) 2417.

35. Boltaks, B., Mokhov, Yu, "Self Diffusion and Diffusion of Impurities in Lead Telluride and Lead Selenide", Zhur. Tekh. Fiz. 28 (1958) 1046.

VII. LIST OF SYMBOLS

a_o	lattice constant
β	temperature coefficient of energy gap, eV/°K.
b	mobility ratio of electrons to holes, u_n/u_p.
C_c	initial concentration, weight percent.
C	concentration at any point in specimen, weight percent.
E	energy gap at a given temperature, eV.
E_o	energy gap at absolute zero, eV.
e	charge on electron = 4.8×10^{-10} esu.
eV	energy in electron volts.
g	fraction of ingot solidified.
$\underline{k}$	wave number of an electron, cm^{-1}.
k	Boltzman constant = 8.61×10^{-5} eV/°K.
k_c	solid to liquid solute concentration ratio, at equilibrium.
m	electronic mass = 9.1×10^{-28} grams.
m_p	effective hole mass in the lattice, grams.
m_n	effective electronic mass in the lattice, grams.
n	number of electrons per cubic centimeter of solid.
N_a	number of acceptor impurity atoms/cm^3.
n_i^2	equilibrium product of electrons and holes at a temperature T.
u_n	mobility of electrons, cm^2/V-sec.
u_p	mobility of holes, cm^2/V-sec.
p	number of holes per cubic centimeter of solid.
Q	Seebeck coefficient. stat volts/°K.
r	ratio ρ_e/ρ_o

R	Hall coefficient, cm^3/coulomb.
ρ	electrical resistivity ohm-cm.
ρ_e	resistivity at intersection of extrinsic and intrinsic resistivity curves.
ρ_o	observed resistivity at the temperature ρ_e determines.
σ	electrical conductivity $ohm^{-1}\text{-}cm^{-1}$.
θ	Bragg angle.

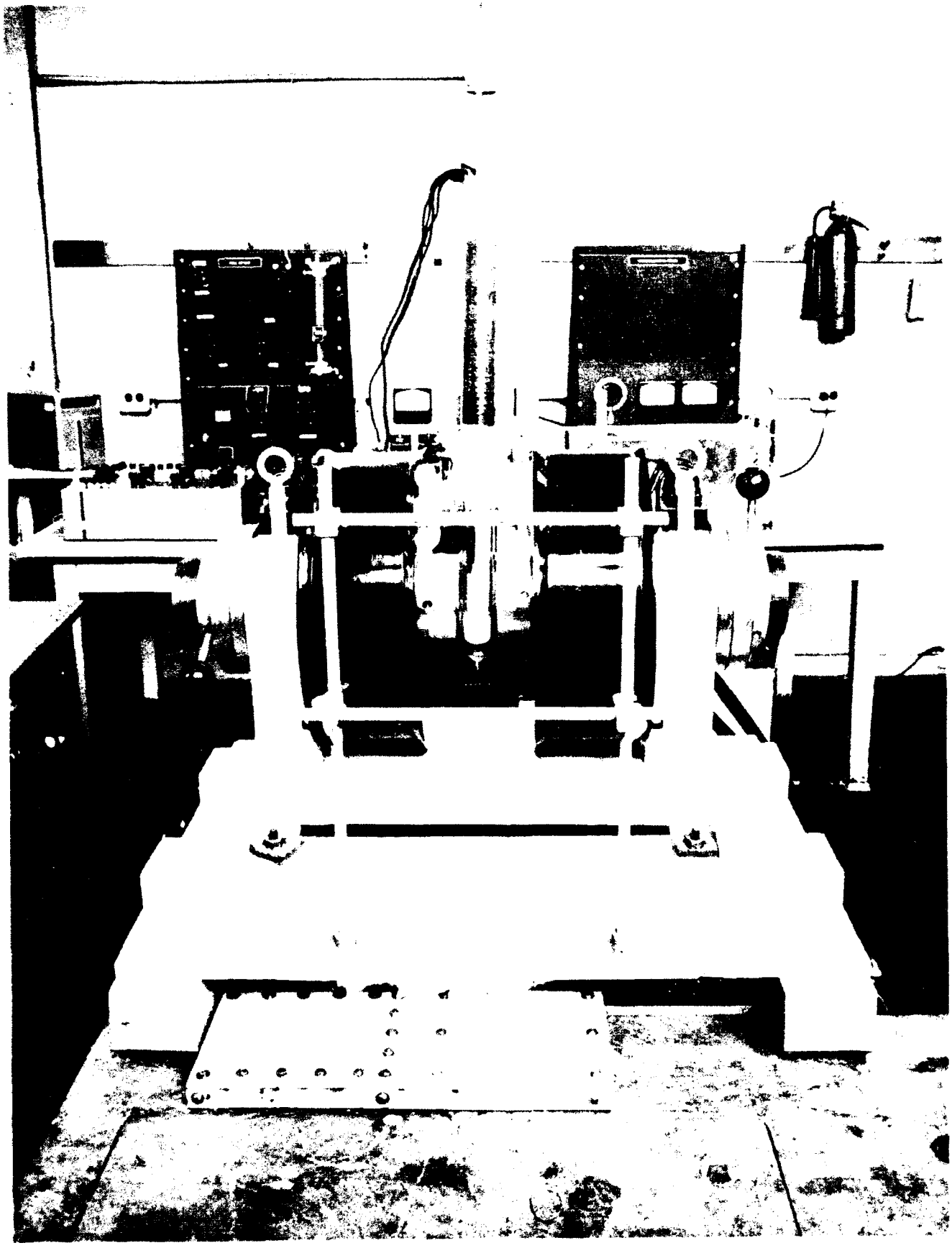

Fig. 1 Hall Effect Apparatus

AD _____

NEW YORK UNIVERSITY, N.Y. - STOICHIOMETRY AND ELECTRONIC PROPERTIES OF PbTe by E. Miller, K. K. Komarek, I. B. Cadoff December 1959, 52 p. incl. illus. and tables. (Project 7021; Task 70661)(WADC TR 59-570) (Contract AF 33 (616)-3883) Unclassified report

Off-stoichiometric single crystals of PbTe were grown by the Bridgman technique at a solidification rate of 0.35 cm/hr. At this low solidification rate the crystals were longitudinally segregated, the composition at any point corresponding to that dictated by the solidus curve of the phase diagram. The phase diagram shows that PbTe has an off-stoichiometric melting point; the difference in concentration between the maximum melting point and the stoichiometric point being 0.002 atomic percent, with the congruent melting point on the tellurium rich side of the stoichiometric point. Stoichiometric PbTe is in equilibrium with liquid 0.41 weight percent rich in lead, the equilibrium temperature being 923.2°C. The solubility of both lead and tellurium in PbTe is restricted, the maximum lead and tellurium excess being 5×10^{19} atoms/cm^3. The crystals were cut into thin sections perpendicular to the growth direction and the slices homogenized to yield samples of different impurity concentrations of lead or tellurium. Resistivity, Hall coefficient, and thermoelectric power measurements were made as a function of temperature on three slices corresponding to stoichiometric, excess lead, and excess tellurium. High-temperature measurements could be made reproducibly with no loss of tellurium by coating the sample with Sauereisen No. 10, a room-temperature hardening cement. The results obtained were analyzed for the basic electronic parameters of the material. The high temperature results were brought into agreement with room temperature optical absorption data after correcting for vacancy generation at elevated temperatures. The energy gap at absolute zero was calculated to be 0.24 eV, and has a temperature variation of $+ 2.5 \times 10^{-4}$ eV/°K. The mobility ratio is $2.2 + 0.15$ and the electron and hole room temperature mobilities are 1170 and 500 cm^2/ volt-sec respectively. The electronic effective mass was found to be 0.22 m and the hole effective mass 0.29 m.

UNCLASSIFIED

AD _____

NEW YORK UNIVERSITY, N.Y. - STOICHIOMETRY AND ELECTRONIC PROPERTIES OF PbTe by E. Miller, K. K. Komarek, I. B. Cadoff December 1959, 52 p. incl. illus. and tables. (Project 7021; Task 70661)(WADC TR 59-570) (Contract AF 33 (616)-3883) Unclassified report

Off-stoichiometric single crystals of PbTe were grown by the Bridgman technique at a solidification rate of 0.35 cm/hr. At this low solidification rate the crystals were longitudinally segregated, the composition at any point corresponding to that dictated by the solidus curve of the phase diagram. The phase diagram shows that PbTe has an off-stoichiometric melting point; the difference in concentration between the maximum melting point and the stoichiometric point being 0.002 atomic percent, with the congruent melting point on the tellurium rich side of the stoichiometric point. Stoichiometric PbTe is in equilibrium with liquid 0.41 weight percent rich in lead, the equilibrium temperature being 923.2°C. The solubility of both lead and tellurium in PbTe is restricted, the maximum lead and tellurium excess being 5×10^{19} atoms/cm^3. The crystals were cut into thin sections perpendicular to the growth direction and the slices homogenized to yield samples of different impurity concentrations of lead or tellurium. Resistivity, Hall coefficient, and thermoelectric power measurements were made as a function of temperature on three slices corresponding to stoichiometric, excess lead, and excess tellurium. High-temperature measurements could be made reproducibly with no loss of tellurium by coating the sample with Sauereisen No. 10, a room-temperature hardening cement. The results obtained were analyzed for the basic electronic parameters of the material. The high temperature results were brought into agreement with room temperature optical absorption data after correcting for vacancy generation at elevated temperatures. The energy gap at absolute zero was calculated to be 0.24 eV, and has a temperature variation of $+ 2.5 \times 10^{-4}$ eV/°K. The mobility ratio is $2.2 + 0.15$ and the electron and hole room temperature mobilities are 1170 and 500 cm^2/ volt-sec respectively. The electronic effective mass was found to be 0.22 m and the hole effective mass 0.29 m.

UNCLASSIFIED

AD _____

NEW YORK UNIVERSITY, N.Y. - STOICHIOMETRY AND ELECTRONIC PROPERTIES OF PbTe by E. Miller, K. K. Komarek, I. B. Cadoff December 1959, 52 p. incl. illus. and tables. (Project 7021; Task 70661)(WADC TR 59-570) (Contract AF 33 (616)-3883) Unclassified report

Off-stoichiometric single crystals of PbTe were grown by the Bridgman technique at a solidification rate of 0.35 cm/hr. At this low solidification rate the crystals were longitudinally segregated, the composition at any point corresponding to that dictated by the solidus curve of the phase diagram. The phase diagram shows that PbTe has an off-stoichiometric melting point; the difference in concentration between the maximum melting point and the stoichiometric point being 0.002 atomic percent, with the congruent melting point on the tellurium rich side of the stoichiometric point. Stoichiometric PbTe is in equilibrium with liquid 0.41 weight percent rich in lead, the equilibrium temperature being 923.2°C. The solubility of both lead and tellurium in PbTe is restricted, the maximum lead and tellurium excess being 5×10^{19} atoms/cm^3. The crystals were cut into thin sections perpendicular to the growth direction and the slices homogenized to yield samples of different impurity concentrations of lead or tellurium. Resistivity, Hall coefficient, and thermoelectric power measurements were made as a function of temperature on three slices corresponding to stoichiometric, excess lead, and excess tellurium. High-temperature measurements could be made reproducibly with no loss of tellurium by coating the sample with Sauereisen No. 10, a room-temperature hardening cement. The results obtained were analyzed for the basic electronic parameters of the material. The high temperature results were brought into agreement with room temperature optical absorption data after correcting for vacancy generation at elevated temperatures. The energy gap at absolute zero was calculated to be 0.24 eV, and has a temperature variation of $+ 2.5 \times 10^{-4}$ eV/°K. The mobility ratio is $2.2 + 0.15$ and the electron and hole room temperature mobilities are 1170 and 500 cm^2/ volt-sec respectively. The electronic effective mass was found to be 0.22 m and the hole effective mass 0.29 m.

UNCLASSIFIED